Study of the relationship between red wine colloidal fraction and astringency by asymmetrical flow field-flow fractionation coupled with multi-detection

Kevin Pascotto, Coline Leriche, Soline Caillé, Frédéric Violleau, Jean-Claude Boulet, Olivier Geffroy, Cécile Levasseur-Garcia, Veronique Cheynier

Study of the relationship between red wine colloidal fraction and astringency by Asymmetrical Flow Field-Flow Fractionation coupled with multi-detection

Kevin Pascotto[a,b], Coline Leriche[e], Soline Caillé[c], Frédéric Violleau[a,b], Jean-Claude Boulet[c,d], Olivier Geffroy[a], Cécile Levasseur[a] and Véronique Cheynier[c]

[a] Plateforme TFFFC, Université de Toulouse, INP-PURPAN, Toulouse, France

[b] Laboratoire de Chimie Agro-industrielle, LCA, Université de Toulouse, INRAE, Toulouse, France

[c] SPO, INRAE, Univ Montpellier, Institut Agro, Montpellier, France

[d] INRAE, PROBE Research Infrastructure, Polyphenol Analytical Facility, Montpellier, France

[e] INRAE, UE999 Pech-Rouge, Gruissan, France

Abstract

Macromolecules including condensed tannins and polysaccharides impact wine taste and especially astringency. Asymmetrical Flow-Field-Flow-Fractionation (AF4) coupled to UV detection (UV), multi-angle light scattering (MALS) and refractive index detection (dRI) has been proposed to separate red wine colloids.

The present work aimed at relating AF4-mutidetection profiles with red wine astringency. Fifty commercial red wines characterized by a trained sensory panel were analysed by AF4-UV-MALS-dRI and UV-visible spectroscopy. The analytical data set was built by selecting the three variables most predictive of the astringency score from each table (UV, dRI, MALS, M_w distribution, and UV-visible spectra of whole wine, permeate and retentate A4F fractions) and analysed by principal component analysis. Red wine astringency was more related to variables extracted from the AF4 data than to UV-absorbance of the wine or permeate, confirming the relevance of AF4-multidetection for analysis of the colloidal fraction involved in this perception.

Key words: wine, astringency, polyphenols, macromolecules, AF4-UV-MALS-dRI, chemometrics

1. Introduction

Astringency is one of the major sensory attributes of red wines. It is defined as dryness, tightening, and puckering sensations perceived in the oral cavity during the intake of astringent compounds (Soares et al., 2020). Polyphenolic compounds and especially tannins are known to be involved in red wine astringency (Gawel, 1998). This perception is generally attributed to the capacity of tannins to bind salivary proteins, leading to the formation of precipitates which reduce the lubrication in the mouth (Bate-Smith, 1973; Baxter, Lilley, Haslam, & Williamson, 1997; McRae & Kennedy, 2011).

Perceived astringency increases with tannin molecular weight (degree of polymerization) (Peleg, Gacon, Schlich, & Noble, 1999; Vidal et al., 2003), their number of galloyl substituents (galloylation degree) (Vidal et al., 2003) and their concentration (Vidal, Courcoux, et al., 2004). Red wine astringency was reported to be primarily associated with a fraction containing higher molecular weight phenolics (> 5 kDa) (Hufnagel & Hofmann, 2008a, b) although some lower molecular weight phenolics (e.g. phenolic acids and their ethyl esters, flavan-3-ol monomers and oligomers, flavonol and dihydroflavonol glycosides) also exhibited astringency (Ferrer-Gallego, Hernández-Hierro, Rivas-Gonzalo, & Escribano-Bailón, 2014; Hufnagel & Hofmann, 2008b; Peleg et al., 1999; Vidal et al., 2018).

Polysaccharides constitute another important group of wine macromolecules (Pellerin, Vidal, Williams & Brillouet, 1995). They comprise polysaccharides rich in arabinose and galactose (PRAGs), and rhamnogalacturonan II (RGII) originating from grape cell walls (Pellerin, Vidal, Williams, & Brillouet, 1995), and mannoproteins (MPs) from yeast cell walls. These compounds are known to interact with tannin perception, reducing astringency both in model solutions (Le Bourvellec & Renard, 2012; Vidal et al., 2004), and in red wines (Boulet et al., 2016; Quijada-Morín, Williams, Rivas-Gonzalo, Doco, & Escribano-Bailón, 2014).

Astringency perception results from a complex system involving multiple factors. Some works based on chemometrics approach modelled analytical data to explain the sensory impact of chemical compounds, considering many factors. Several authors used multivariate analysis (Quijada-Morín et

al., 2014) such as multiple linear regression (MLR) (Boulet et al., 2016; Quijada-Morín et al., 2014), or partial least squares regression (PLSR) (Preys et al., 2006), to cross instrumental and sensory data for describing the relationships between several groups of variables. For example, the smoothing capacity of wine polysaccharides was confirmed using chemometrics tools (principal component analysis, PCA and multiple linear regression, MLR) (Boulet et al., 2016; Quijada-Morín et al., 2014). Additionally, it was shown that the absorbance values at $\lambda = 230$ nm efficiently predict the perceived astringency in wine (Boulet et al., 2016). However, these studies did not consider the apparent molar mass of compounds. Other works assessed the impact of individual phenolic compounds quantified by HPLC-DAD (Kallithraka, Kim, Tsakiris, Paraskevopoulos, & Soleas, 2011) and HPLC-DAD-MS (Vidal et al., 2018). Nevertheless, neither higher molecular weight polyphenols nor polysaccharides were considered in their models. Tannin composition is classically determined by HPLC after depolymerisation in the presence of a nucleophilic reagent (e.g. thiolysis, phloroglucinolysis). However, when applied to wine, these methods do not predict astringency unlike more global methods such as BSA precipitation (Boulet et al., 2016; Harbertson & Kennedy, 2002), or spectrophotometric measurements (Boulet et al., 2016).

A method based on Asymmetrical – Flow – Field – Flow – Fractionation (AF4), coupled to a multi-detection system consisting of UV detection (UV), multi-angle light scattering (MALS), and differential refractometer index (dRI) (AF4-UV-MALS-dRI), using a wine like solution as the mobile phase has been recently developed (Pascotto, Cheynier, Williams, Geffroy, & Violleau, 2020). This method allowed separation of wine macromolecules into four fractions. The first three were assigned to higher M_w tannins coeluted with lower M_w polysaccharides such as rhamnogalacturonan II (F1), to intermediate M_w polysaccharides such as polysaccharides rich in arabinan and galactan (PRAGs) (F2), and to higher M_w mannoproteins (F3) whereas the last fraction (F4) was not identified (Pascotto et al., 2020). Moreover, Marassi and coworkers reported the presence of residual proteins in the low retention time fractions (Marassi et al., 2021).

The hypothesis of the present study was that the AF4 multi-detection profiles obtained with the method developed in our earlier paper (Pascotto et al., 2020) are related to red wine astringency. To

evaluate whether the method is relevant to analyse the wine colloids contributing astringency (i.e. tannins) or mitigating it (e.g. polysaccharides), AF4 analysis was performed on a series of red wines from Languedoc region (France) which were tasted by a sensory panel using QDA procedure. The two data sets (analytical and sensory) were then processed using multiway analysis to assess the potential of A4F profiles for prediction of wine astringency and determine the contribution of the different A4F fractions.

2. Materials and methods

2.1. Wine collection

In this work, fifty red wines produced in 2016 in several Protected Denominations of Origin (PDOs) from the French Languedoc area (Corbières-Boutenac, la Clape, Faugères, Minervois-Terrasses de l'Argent Double, Languedoc-Montpeyroux and Pic-Saint-Loup) were used. Most of the samples were blended wines mainly made from Grenache, Syrah and Carignan and are sold between 5 and 20 euros. Wines from the PDO Corbières-Boutenac were barrel aged. Wines were coded 1 to 50 as summarized in Table S1. Fifteen bottles of each wines were used for the sensory analysis, one bottle for the chemical analysis.

2.2. Sensory analysis

The wines were evaluated using Quantitative Descriptive Analysis (Stone & Sidel, 2004) QDA® in 2019 by a trained panel from the Sensory Laboratory of UMR SPO, INRAE (Montpellier, France). This panel was composed of 18 judges unrelated to the wine industry (genders: 12 women, 6 men; average age: 55 years old; seniority on the panel: 5 years in average - 3 months minimum - 13 years maximum). The selection of these judges was based on their sensory performances and their ability to communicate in group (Depledt, 2009; Nicod, 1998). After three sessions for vocabulary generation on the 50 wines, the panel considered 16 independent and discriminating descriptors, including astringency (Depledt, 2009). Judges were trained during a one-hour session on the perception of astringency. A grape seed and stalk tannin extract was added to wine sample as a training standard for astringency assessment. A range of concentrations was presented to the panel: 0 – 0.6 and 0.8 $g.L^{-1}$,

and the judges were asked to classify these samples according to the astringency intensity. As a final training step, a Feedback Calibration Method was used in order to check if the panel performances were strong enough to characterize the wines efficiently (Findlay, Castura, Schlich, & Lesschaeve, 2006). For the rating, wines were presented in a monadic service according to a Latin square of Williams (Macfie, Bratchell, Greenhoff, & Vallis, 1989), served in black glasses, at room temperature with a plastic cup over glasses to keep aromas. Judges evaluated the wines in standard tasting cabs and rated the intensity of each descriptor on linear scales, from low corresponding to absence of perception to high corresponding to very intense perception, for each wine. The distances on the linear scale are then converted to scores (from 0 to 10) for statistical analyses. Judges were invited to rinse their mouth with a solution of pectin (1 $g.L^{-1}$) then with water between each sample in order to limit the carry over effect of astringency of red wines (Colonna, Adams & Noble, 2004). Six sessions were dedicated to the rating: one session for each PDO. At the end, the repeatability of the panel was tested independently, considering two wines from each PDO, with a repetition in the same session. Astringency intensities were then extracted from the QDA data.

2.3. AF4 analysis

2.3.1. Chemical

Ultrapure water was obtained from a Merck MilliQ integral 15 system. Ethanol, methanol, formic acid and HCl (99% purity, HPLC grade) were purchased from Carlo Erba (France). Sodium azide and sodium nitrate (99.5% purity) were purchased from Sigma Aldrich (St Louis, MO, USA). Potassium sulphate was obtained from Merck (Darmstadt, Germany) and has a purity at 99%. Bovine serum albumin (BSA) was purchased from Thermo Scientific (USA) and prepared at 2 mg/ml in a 0.9% NaCl solution (m/v).

2.3.2. Sample preparation

Wine aliquots (1 mL) were dried with a Genevac EZ-2plus evaporator under reduced pressure at 8 mbars at 40°C and stored at -80 °C until used to limit evolution. Then, dried wine was dissolved in 1 mL of a wine like solution (water/ethanol – 88/12, v/v) with a pH adjusted to 3.5 by adding formic

acid. The resulting mixture was ultrasonically mixed for 5 min, vortexed and then centrifuged at 3000 g for 5 min to remove any precipitate.

2.3.3. Instrumentation, elution conditions and molecular weight calculation

The instrumental set-up and AF4 methods used for this work are the same as described earlier (Pascotto et al., 2020). In brief, a Thermo Scientific Ultimate 3000 HPLC System, including degasser, isocratic pump and autosampler, was used to inject samples and transport the mobile phase through the system. The pump was coupled with the Eclipse AF4 (Wyatt Technology) to regulates flows in the AF4 separation channel (long channel, Wyatt Technology Europe, Germany). The height of inserted spacer of the AF4 channel was 350 µm and the membrane (Consenxus, Germany) was in cellulose material with a cut-off at 5 kDa. A multi-detection system including a UV-visible (set at λ = 280 and 230 nm), MALS, and a dRI, detectors (Wyatt Technology) was coupled with the AF4 system. Chromeleon 6.8 software was used to control autosampler, pump and Eclipse flows. Acquisition of UV, MALS and dRI data was performed using the Astra 6.1 software. Mobile phase used was composed of 88% water (v/v) and 12% ethanol (v/v). Formic acid was added to adjust pH at 3.5. A potassium salt was incorporated at 1 $g.L^{-1}$ (K^+ equivalent) and 0.02% of sodium azide (s/v) was also added to inhibit bacterial development. Wine samples were loaded to 400 µL in the AF4 channel. The programs used to the wine sample and blank started with two minutes with the inlet flow at 1 $mL.min^{-1}$ to obtain the baseline. Then, the relaxation step was applied for 8 min, against 6 min in the previous paper (Pascotto et al., 2020). During this step, both the inlet and outlet channel flows were maintained constant, at 1 $ml.min^{-1}$ and 3 $mL.min^{-1}$, respectively. Then, the elution step was started with a crossflow (Q_c) = 3 $mL.min^{-1}$, which was decreased exponentially (following equation 1) over time to 0.04 $mL.min^{-1}$ and then maintained constant for 25 min.

$$Q_c(time) = Q_c^{end} + \left(Q_c^{start} - Q_c^{end}\right)e^{\frac{-time}{5}} \quad (1)$$

where, Q_c^{start} is the crossflow rate at the beginning of the elution step (3 $mL.min^{-1}$), and Q_c^{end} is the final crossflow rate targeted (0.04 $mL.min^{-1}$). Each wine sample was preceded by a blank injection and was followed by a cleaning program, injecting 100 µL of a solution of water/methanol (50:50) before the next injection.

The weight average molecular weight (M_w) was calculated as described earlier (Pascotto et al., 2020). Briefly, the M_w of compounds eluted in the F1 fractions was calculated using the dn/dc value reported for tannins: 0.247 (Vernhet et al., 2011). Those of compounds eluted in fractions F2 and F3 were calculated using the *dn/dc* value reported for polysaccharides, PRAGs and MPs: 0.146 (Redgwell, Schmitt, Beaulieu, & Curti, 2005).

2.4. Calculation of the polyphenol recovery rate by spectrophotometry

The permeate fraction was recovered at the outlet of the crossflow during the relaxation step, using a fraction collector AFC – 3000 (Thermo Scientific). Additionally, the retentate fraction was also recovered during the elution step at the outlet-flow using a fraction collector Frac920, GE-Healthcare, Sweden), positioned after the AF4 detectors. The permeate and retentate fractions were taken to dryness with a Genevac EZ-2plus evaporator under reduced pressure at 8 mbars at 40 °C and freeze dried. Then, both permeate and retentate dry powders were solubilized in 50 mL and 1 mL respectively while the whole wine was diluted 200-fold in HCl (2%). Obtained sample solutions were distributed in 96 wells (UV plate, Corning Life Sciences) and wells were filled with 170 µL of the sample. UV-visible absorbance was measured using a Nanoquant Infinite® 200 Pro spectrophotometer (Tecan, Switzerland). Then, UV-visible spectra were acquired with 1 nm step, over the range 230 – 600 nm for each fraction and for the whole wine. Absorbance values at λ = 280 nm (A280) and at λ = 230 nm (A230) were extracted from the retentate and permeate fractions and the whole wine spectra. The percentage of both A280 and A230 of the retentate and permeate fractions were calculated from the absorbance values of the whole wine, representing 100% of the sample. Thus, the percentage of recovery of the UV absorbing material was estimated for each analysis at 280 and 230 nm.

2.5. Data processing

2.5.1. Sensory data

The performances of the panel and of each judge were first evaluated. A three-way ANOVA with interactions (Y = Wine + Judge + Repetition + Wine x Judge + Wine x Repetiton + Judge x Repetition + ε with α=5%) and a Generalized Products Analysis (GPA) were performed to assess the repeatability

of the judgements and to check the three main performances of a trained panel: discrimination, consensus, and repeatability (Depledt, 2009). Both statistical treatments confirmed that the panel fulfilled these requirements. Then, the data were treated to create groups of wines according to their astringency intensity. First, a two-way ANOVA (Y = Wine + Judge + ε with α=5%) and a difference test (Fisher, LSD with α=5%) were performed to discriminate wines. Wines were separated into three groups according to their mean score of astringency and the significant differences shown by the Fisher-LSD test. First, thanks to the Fisher-LSD test, extreme samples, showing the lowest and the highest astringency intensity were identified. Then, groups were created from this first observation, the high intensity group was composed of wines non significantly different from the highest intensity sample but significantly different from the lowest intensity one, and vice versa for the low intensity group. Samples belonging to none of these groups were gathered in an intermediate intensity group.

2.5.2. Cross-tabulation of the sensory and analytical data

The analytical data obtained from the above-described methods were gathered in eight ***X*** tables, while astringency scores were collected in the ***Y*** matrix (Table 1). The first eight minutes corresponding to the elution step of the AF4 profiles were truncated to remove the unnecessary variables. Then, each table was smoothed using a second-degree polynomial, 0-order. Due to the large number of variables contained in the eight tables forming the ***X*** matrix, three variables were selected step by step from each ***X*** table on the basis of their covariance with the astringency score (***Y*** tables), using the *CovSel* procedure (Roger, Palagos, Bertrand, & Fernandez-ahumada, 2011), under Chemflow web application (https://vm-chemflow-francegrille.eu/) and were concatenated under $\boldsymbol{X}_{sel}$ table (Table 2). In addition, both values of the percentage of retentate and permeate at 280 and 230 nm (%R280, %R230 and %P280, %P230, respectively), were added to this table, independently to the *CovSel* procedure (Table 2). Then, principal component analysis (PCA) was performed under R, version 4.0.2, using factoextra package, from $\boldsymbol{X}_{sel}$ table.

3. Results and discussion

3.1. Sensory analysis

Quantitative Descriptive Analysis allowed discrimination of three groups of wines according to their astringency. The ANOVA highlighted significant differences for the descriptor astringency (p-value<0.001). Moreover, the fisher-LSD test also allowed to discriminate three groups (Fig.1): one constituted by wines having a mean astringency score below 6.00 ("Low astringency samples" or LAS); a second group having a score between 6.00 and 7.50 ("Medium astringency samples" or MAS) and a third group of wines having a score over 7.50 ("High astringency samples" or HAS).

3.2. Chemical data analysis

3.2.1. Polyphenol recovery rate by spectrophotometry

Fig. 2 shows the distribution of recovery calculated over the 50 wine samples, for the permeate (%P), the retentate (%R) and the sum of these two fractions, at 230 and 280 nm. Most of UV-absorbing material of samples was removed through the channel membrane and recovered in the permeate (Fig. 2a, d) and the amount recovered in the retentate (%R) corresponded to ~2% for both wavelengths (Fig. 2b, e). Moreover, %P appeared lower at 230 nm (mean ~ 80%) than at 280 nm (~ 88%) whereas the retained fraction (%R) seems to be slightly higher when measured at 230 nm than at 280 nm. These two results suggest that the higher molecular mass UV-absorbing material can be distinguished from the fraction eliminated in the permeate, by a shift of the maximum of absorbance. Furthermore, the total recovery percentage was higher at 280 nm than at 230 nm, suggesting that the losses after separation (through absorption on the membrane and/or during sample preparation and injection), concern more the higher molecular weight compounds.

*3.2.2. Description of UV-vis spectra and AF4 fractograms (**X** tables)*

The UV-visible spectra of the whole wines, the permeate and retentate fractions are presented in Fig. 3a to 3c. The LAS, MAS and HAS astringency groups can be distinguished according to their absorbance spectra showing low, intermediate, and high intensities, respectively, along the entire spectrum for the retentate fractions and at lower wavelengths only for the entire wines. This suggests that the retentate contains higher molecular weight phenolics that are astringent. The higher

239 absorbance values observed in the range 254-600 nm for the wine and permeate spectra reflect the
240 presence of phenolic compounds such as anthocyanins, flavonols, and phenolic acids which contribute
241 little to astringency and are recovered mostly in the permeate. Wine absorbance values at 230 nm also
242 appeared related to the astringency group, confirming earlier findings (Boulet, Ducasse, & Cheynier,
243 2017; Boulet et al., 2016).

244 The AF4 profiles of the 50 wines obtained with the three detectors and the molar mass distribution
245 (Figs. 3d to 3h) show the presence of several fractions as described earlier (Pascotto et al., 2020). The
246 first one (F1), eluted between two and five minutes, is clearly visible on the UV and dRI fractograms
247 and to a lesser degree on the MALS fractogram. It corresponds to higher molecular weight tannins
248 coeluted with RGII. Overall, the abundance of this fraction, especially in the UV profiles recorded at
249 280 nm (Fig. 3d) and 230 nm (Fig. 3e) increases in relation with the astringency level of wine,
250 consistent with the known contribution of higher molecular weight tannins to wine astringency.
251 Furthermore, RG-II has been shown to reduce perception of tannin astringency both in model solution
252 (Vidal et al, 2004) and in wine (Boulet et al, 2017), However, astringency seems mostly related to the
253 intensity of the UV signal and thus to the tannin concentration in F1, so that the effect of RGII cannot
254 be determined. Fractions (F2 and F3) are mostly visible on the MALS and dRI fractograms (Figs. 3f,
255 3g). These fractions, eluted between five and eight minutes and between eight and fifteen minutes,
256 respectively, have been attributed to intermediate (F2) and higher (F3) M_w polysaccharides (Pascotto
257 et al., 2020).

258 Moreover, the presence of UV absorbing material in these fractions could reflect the presence of
259 proteins or of polyphenols interacting with the polysaccharidic material. However, no relationship was
260 observed between the astringency level and their peak intensity or retention time. The fourth fraction
261 (F4) clearly visible on the MALS fractogram was eluted between fifteen and thirty minutes (Fig. 3f).
262 A great variability was observed from one sample to another for F4. It can be assumed that this
263 fraction was present in very small amount because the corresponding dRI or UV signal were close to
264 the baseline. Therefore, M_w could not be calculated for this fraction. However, the radius of gyration
265 (R_g) was determined from the MALS data and ranged from ~ 60 to 100 nm (data not shown). In

addition, for some samples, the MALS fractograms exhibited a fifth fraction (F5), eluting between 30 and 50 minutes, with a R_g = ranging from ~ 80 to 120 nm. Finally, the mean M_w calculated for F1, F2 and F3 varied between 7.5 and 23 kDa (F1), between 62 and 135 kDa (F2) and between 160 and 600 kDa (F3), respectively (Fig. 3g). The M_w of F1 increased with the astringency level while no clear relationship was found for F2 and F3.

3.3. Correlation between sensory and chemical data using multivariate analysis

3.3.1. Variable selection

To avoid biases due to the huge number of variables in each spectrum or profile and high correlations between them when performing PCA, three variables were independently selected from each ***X*** table, on the basis of their correlation with the wine astringency scores, using the *CovSel* procedure (Roger et al., 2011), as summarised in Table 2 and Fig. S1. The 230 nm wavelength was selected in all UV spectra (retentate, permeate and whole wine), confirming the good potential of this wavelength to predict the astringency scores (Boulet et al., 2016). However, the other wavelengths selected differed according to the fraction. Indeed, a wavelength around 280 nm (277 nm) was only selected from the retentate fraction spectra. It can be attributed to higher molecular weight tannins retained over the A4F membrane which are known to be major contributors of wine astringency (Boulet et al., 2016; Hufnagel & Hofmann, 2008a).

Other polyphenols such as anthocyanins, flavonols, and phenolic acids, contribute highly to the wine absorbance around 280 nm (Boulet et al., 2017) but they were recovered mostly in the permeate. Absorbances at 317 and 523 nm, reflecting the presence of phenolic acids and of anthocyanins, respectively, were selected as the most relevant variables for astringency prediction in the permeate spectra. Anthocyanins have been reported to increase wine astringency (Brossaud, Cheynier, & Noble, 2001) and interact with salivary proteins (Ferrer-Gallego et al., 2015). Phenolic acids have been reported to contribute to astringency (Ferrer-Gallego et al., 2014; Hufnagel & Hofmann, 2008a; Peleg et al., 1999; Vidal et al., 2018) and prediction of wine astringency was improved when taking their concentration into account (Boulet et al., 2016). Absorbance at 313 nm selected in the wine spectra also corresponds to phenolic acids or to coumaroylated anthocyanins.

These anthocyanins show higher affinity toward PVPP than non-acylated ones (Gil et al., 2017), suggesting that they may be more astringent. Moreover, the 245 nm wavelength was selected in the spectra of both whole wines and retentates among the variables most correlated with astringency. In contrast, it was not selected in the permeate fraction (Table 2). This suggests that compounds associated with absorbance at 245 nm, whose nature remains to be determined, do not have a major impact on astringency when present as monomers or oligomeric molecules but contribute more strongly when they are involved in larger polymers. Two variables selected from the 280 nm-UV fractogram were localised in F1 and one in F2 (Table 2, Fig. S1), indicating that this data provided information related to both the presence of tannins and of tannins interacting (or coeluted) with the medium molecular mass polysaccharides such as PRAGs. However, all three variables selected from the 230 nm-UV fractogram were in F1 (Table 2, Fig. S1). In contrast, the variables selected from the MALS fractogram, were rather located in fractions F2/F3 and F4 (Table. 2, Fig. S1). This indicates that this table brought variables related both to polysaccharidic compounds (F2/F3), and to unknow compounds contained in F4, to explain the astringency scores.

Further, the variables selected from both dRI and M_w tables concern both fractions of tannins/RGII and fractions containing polysaccharidic compounds (Table. 2, Fig. S1). Two variables relating to F1 and one to F3 were selected from the dRI table and one variable relating to the mass of F1 and two relating to the masses of polysaccharides from the M_w table.

3.3.2. Principal component analysis (PCA)

Fig. 4 shows the distribution of individuals, coloured according to the astringency groups (a), and of the quantitative variable groups (correlation circle, b) on the first plane of the PCA performed using the variables selected from all tables. HAS wines were well separated from LAS wines along PC1 which was the component most influenced by the astringency groups (Fig 4a), Moreover, LAS appeared better grouped compared to HAS or MAS, suggesting that these samples had more similarity regarding analytical characteristics compared to other groups. Projection of variables on the correlation circle (Fig 4b), shows that HAS were characterized with higher values of UV absorbance of the retentate, variables associated to F1 in the AF4 fractograms (M_w at 3.7 min, dRI at 2.8 and 3.4

min, UV-280 and 230 nm at 3.2, 3.5, 3.8 min and 3.3, 3.8 respectively) and by the higher values of recovery (%R at 280 and 230 nm).

These observations suggest that the abundance of F1 and the M_w of this fraction (compounds > 5 kDa) increased substantially the perceived astringency in wine, as proposed earlier (Boulet et al., 2016). Furthermore, the UV-280 nm variable selected at 7 min of retention time (corresponding to F2), was also positively correlated to PC1, indicating that F2 from HAS absorbs highly in UV. F2 was already identified to correspond to polysaccharidic fractions (Pascotto et al., 2020). This suggests that F2 in HAS also contains very high molecular weight tannins. In contrast, LAS showed higher values of variables related to F2/F3 (LS-9.2 min, Mw-9.6, and Mw- 13.0 min, dRI-8.2 min) and F4 (LS-21.7 and LS 26.9). This indicates that perceived astringency is counteracted by the polysaccharidic material, as shown earlier (Boulet et al., 2016; Quijada-Morín et al., 2014), but also by the compounds eluted in F4 which are not yet identified. In addition, it is interesting to note that the impact of polysaccharides seems to increase with their M_w (Fig. 4b). Moreover, LAS were also the samples having the highest absorbance values of permeate at 230 and 280 nm (%P230 and %P280). This observation is consistent with the above discussed results showing that the most astringent wines had the highest percentage of recovery (R%). MAS were highly dispersed and overlapped with both HAS and LAS categories.

Two ways were envisaged. (i): This variability can be explained as the mean astringency scores, determined by ANOVA were not significantly different from the other two groups. (ii): the presence of proteins in the earlier retention time fractions, corresponding to F1 in this work, has been recently shown (Marassi et al., 2020) and may contribute to the high intensity of F1 in UV absorbance. On the other hand, PC2, was positively associated with absorbance values of the permeate fraction at 317 and 523 nm and of the wine, especially at 313 nm, but also to variables associated to the F4 fraction (LS-21.7 and LS 26.9). Absorbance values at 313, 317, and 523 nm do not contribute to PC1 although they have been selected on the basis of their correlation with the astringency scores, indicating that their contribution to wine astringency is actually negligible compared to that of larger molecular weight phenolic compounds eluted in F1. Furthermore, the whole wine wavelength group is relatively well

represented both on PC1 and PC2, meaning that this group of variables contributed to the separation of individuals according to their astringency group (relative to PC1) and the dispersion of individuals on PC2. It confirms that the information contained in the retentate and permeate spectra, which explained the variability of the individuals with respect to PC1 and PC2 respectively, was averaged in whole wines spectra.

Conclusion

Our results show that the profiles obtained on 50 red wines from the French Languedoc- Roussillon region using the AF4-multidetection method described in our previous paper are related to astringency scores determined by a trained sensory panel. The UV absorbing material in the colloid fraction retained by the A4F membrane represented only a few percent of the absorbance measured on the wines. However, red wine astringency was mostly related to retained (> 5kDa) polyphenols and increased with their molecular weight while polyphenols eluted in the permeate fraction, although much more abundant, had a negligible contribution. Lower astringency wines showed higher values of variables related to F2, F3 and F4 in the MALS and M_w profiles, indicating that perceived astringency was counteracted by the polysaccharidic material, in agreement with literature results, but also by unknown compounds eluted in F4. Astringency softening also increased with polysaccharide M_w. The AF4-multidetection method provides the first analysis of the red wine colloids contributing astringency (i.e. higher molecular weight tannins) or mitigating it (i.e. polysaccharides and other unknown polymeric material) in a single run. This paves the way for further investigation of the colloidal material and mechanisms involved in red wine astringency.

Acknowledgments

The authors gratefully acknowledge the funding received from Occitanie Region, France and Ecole d'Ingénieurs Purpan, Toulouse, France for the PhD fellowship of K. Pascotto and from Occitanie Region, France for that of C. Leriche. The union of the Languedoc AOP and the Interprofessional Association of Languedoc Wines are also thanked for providing the wine samples. People involved in

the experiments are gratefully acknowledged, in particular the judges of the sensory panel for their contribution to astringency assessment, the winemakers who supplied the wines used for this work, and D. Kleiber and G. Pasquier for helpful discussions.

Literature cited

Bate-Smith, E. C. (1973). Haemanalysis of tannins: The concept of relative astringency. *Phytochemistry*, *12*(4), 907–912. https://doi.org/10.1016/0031-9422(73)80701-0

Baxter, N. J., Lilley, T. H., Haslam, E., & Williamson, M. P. (1997). Multiple interactions between polyphenols and a salivary proline-rich protein repeat result in complexation and precipitation. *Biochemistry*, *36*(18), 5566–5577. https://doi.org/10.1021/bi9700328

Boulet, J.-C., Ducasse, M.-A., & Cheynier, V. (2017). Ultraviolet spectroscopy study of phenolic substances and other major compounds in red wines: Relationship between astringency and the concentration of phenolic substances. *Australian Journal of Grape and Wine Research*, *23*(2), 193–199.

Boulet, J. C., Trarieux, C., Souquet, J. M., Ducasse, M. A., Caillé, S., Samson, A., Cheynier, V. (2016). Models based on ultraviolet spectroscopy, polyphenols, oligosaccharides and polysaccharides for prediction of wine astringency. *Food Chemistry*. https://doi.org/10.1016/j.foodchem.2015.05.062

Brossaud, F., Cheynier, V., & Noble, A. C. (2001). Bitterness and astringency of grape and wine polyphenols. *Australian Journal of Grape and Wine Research*, *7*(1), 33–39. https://doi.org/10.1111/j.1755-0238.2001.tb00191.x

Colonna A.E, Adams D.O, Noble A.C. (2004). Comparison of procedures for reducing astringency carry-over effects in evaluation of red wines. *Australian Journal of Grape and Wine Research*, *10*(1), 26–31. https://doi.org/10.1111/j.1755-0238.2004.tb00005.x

Depledt Félix, M. J.-L. (2009). *Évaluation sensorielle (3e éd.)*. (Lavoisier Ed. Paris, Ed.).

Ferrer-Gallego, R., Hernández-Hierro, J. M., Rivas-Gonzalo, J. C., & Escribano-Bailón, M. T. (2014).

Sensory evaluation of bitterness and astringency sub-qualities of wine phenolic compounds: Synergistic effect and modulation by aromas. *Food Research International*, *62*, 1100–1107. https://doi.org/10.1016/j.foodres.2014.05.049

Ferrer-Gallego, R., Soares, S., Mateus, N., Rivas-Gonzalo, J., Escribano-Bailón, M. T., & Freitas, V. de. (2015). New Anthocyanin–Human Salivary Protein Complexes. *Langmuir*, *31*(30), 8392–8401. https://doi.org/10.1021/acs.langmuir.5b01122

Findlay, C. J., Castura, J. C., Schlich, P., & Lesschaeve, I. (2006). Use of feedback calibration to reduce the training time for wine panels. *Food Quality and Preference*, *17*(3–4), 266–276. https://doi.org/10.1016/j.foodqual.2005.07.005

Gawel, R. (1998). Red wine astrigency : Rewiev. *Australian Journal of Grape and Wine Research*, 74–95. https://doi.org/https://doi.org/10.1111/j.1755-0238.1998.tb00137.x

Gil, M., Avila-Salas, F., Santos, L. S., Iturmendi, N., Moine, V., Cheynier, V., & Saucier, C. (2017). Rosé Wine Fining Using Polyvinylpolypyrrolidone: Colorimetry, Targeted Polyphenomics, and Molecular Dynamics Simulations. *Journal of Agricultural and Food Chemistry*, *65*(48), 10591–10597. https://doi.org/10.1021/acs.jafc.7b04461

Harbertson James F, Kennedy J.A., Adams D.O. (2002). Tannin in Skins and Seeds of Cabernet Sauvignon , Syrah , and Pinot noir Berries during Ripening, *1*(September 2001), 54–59.

Hufnagel, J. C., & Hofmann, T. (2008a). Orosensory-directed identification of astringent mouthfeel and bitter-tasting compounds in red wine. *Journal of Agricultural and Food Chemistry*, *56*(4), 1376–1386. https://doi.org/10.1021/jf073031n

Hufnagel, J.C., & Hofmann, T. (2008b). Quantitative reconstruction of the nonvolatile sensometabolome of a red wine. *Journal of Agricultural and Food Chemistry*, *56*(19), 9190–9199. https://doi.org/10.1021/jf801742w

Kallithraka, S., Kim, D., Tsakiris, A., Paraskevopoulos, I., & Soleas, G. (2011). Sensory assessment and chemical measurement of astringency of Greek wines: Correlations with analytical

423 polyphenolic composition. *Food Chemistry*, *126*(4), 1953–1958.
424 https://doi.org/10.1016/j.foodchem.2010.12.045

425 Leriche, C., Molinier, C., Caillé, S., Razungles, A., Symoneaux, R., & Coulon-Leroy, C. (2020).
426 Development of a methodology to study typicity of PDO wines with professionals of the wine
427 sector. *Journal of the Science of Food and Agriculture*, *100*(10), 3866–3877.
428 https://doi.org/10.1002/jsfa.10428

429 Macfie, H. J., Bratchell, N., Greenhoff, K., & Vallis, L. V. (1989). Designs To Balance the Effect of
430 Order of Presentation and First-Order Carry-Over Effects in Hall Tests. *Journal of Sensory*
431 *Studies*, *4*(2), 129–148. https://doi.org/10.1111/j.1745-459X.1989.tb00463.x

432 Marassi, V., Marangon, M., Zattoni, A., Vincenzi, S., Versari, A., Reschiglian, P., et al (2021).
433 Characterization of red wine native colloids by asymmetrical flow field-flow fractionation with
434 online multidetection. *Food Hydrocolloids*, *110*, 106204.
435 https://doi.org/10.1016/j.foodhyd.2020.106204

436

437 Mcrae, J. M., & Kennedy, J. A. (2011). Wine and Grape Tannin Interactions with Salivary Proteins
438 and Their Impact on Astringency: A Review of Current Research. *Molecules*, *16*, 2348–2364.
439 https://doi.org/10.3390/molecules16042348

440 Nicod, H. (1998). *L'organisation pratique de la mesure sensorielle, l'entraînement*. (Lavoisier, Ed.)
441 (2nd ed).

442 Pascotto, K., Cheynier, V., Williams, P., Geffroy, O., & Violleau, F. (2020). Fractionation and
443 characterization of polyphenolic compounds and macromolecules in red wine by asymmetrical
444 flow field-flow fractionation. *Journal of Chromatography A*, *1629*.
445 https://doi.org/10.1016/j.chroma.2020.461464

446 Peleg, H., Gacon, K., Schlich, P., & Noble, A. C. (1999). Bitterness and astringency of flavan-3-ol
447 monomers, dimers and trimers. *Journal of the Science of Food and Agriculture*, *79*(8), 1123–

1128. https://doi.org/10.1002/(SICI)1097-0010(199906)79:8<1123::AID-JSFA336>3.0.CO;2-D

Pellerin, P., Vidal, S., Williams, P., & Brillouet, J. M. (1995). Characterization of five type II arabinogalactan-protein fractions from red wine of increasing uronic acid content. *Carbohydrate Research*, *277*(1), 135–143. https://doi.org/10.1016/0008-6215(95)00206-9

Preys, S., Mazerolles, G., Courcoux, P., Samson, A., Fischer, U., Hanafi, M., et al. (2006). Relationship between polyphenolic composition and some sensory properties in red wines using multiway analyses. *Analytica Chimica Acta*, *563*(1-2 SPEC. ISS.), 126–136. https://doi.org/10.1016/j.aca.2005.10.082

Quijada-Morín, N., Williams, P., Rivas-Gonzalo, J. C., Doco, T., & Escribano-Bailón, M. T. (2014). Polyphenolic, polysaccharide and oligosaccharide composition of Tempranillo red wines and their relationship with the perceived astringency. *Food Chemistry*, *154*, 44–51. https://doi.org/10.1016/j.foodchem.2013.12.101

Redgwell, R. J., Schmitt, C., Beaulieu, M., & Curti, D. (2005). Hydrocolloids from coffee: Physicochemical and functional properties of an arabinogalactan-protein fraction from green beans. *Food Hydrocolloids*, *19*(6), 1005–1015. https://doi.org/10.1016/j.foodhyd.2004.12.010

Roger, J. M., Palagos, B., Bertrand, D., & Fernandez-ahumada, E. (2011). Chemometrics and Intelligent Laboratory Systems CovSel : Variable selection for highly multivariate and multi-response calibration Application to IR spectroscopy. *Chemometrics and Intelligent Laboratory Systems*, *106*(2), 216–223. https://doi.org/10.1016/j.chemolab.2010.10.003

Soares, S., Brandão, E., Guerreiro, C., Soares, S., Mateus, N., & De Freitas, V. (2020). Tannins in food: Insights into the molecular perception of astringency and bitter taste. *Molecules*. https://doi.org/10.3390/molecules25112590

Stone and Sidel. (2004). *Quantitative Descriptive Analysis (The QDA method). Sensory evaluation practices*. (C. Elsevier Academic Press, San Diego, Ed.) ((3rd ed.)).

Vernhet, A., Dubascoux, S., Cabane, B., Fulcrand, H., Dubreucq, E., & Poncet-Legrand, C. (2011).

Characterization of oxidized tannins: Comparison of depolymerization methods, asymmetric flow field-flow fractionation and small-angle X-ray scattering. *Analytical and Bioanalytical Chemistry*, *401*(5), 1563–1573. https://doi.org/10.1007/s00216-011-5076-2

Vidal, L., Antúnez, L., Rodríguez-Haralambides, A., Giménez, A., Medina, K., Boido, E., & Ares, G. (2018). Relationship between astringency and phenolic composition of commercial Uruguayan Tannat wines: Application of boosted regression trees. *Food Research International*, *112*(June), 25–37. https://doi.org/10.1016/j.foodres.2018.06.024

Vidal, S., Courcoux, P., Francis, L., Kwiatkowski, M., Gawel, R., Williams, P., et al. (2004). Use of an experimental design approach for evaluation of key wine components on mouth-feel perception. *Food Quality and Preference*, *15*(3), 209–217. https://doi.org/10.1016/S0950-3293(03)00059-4

Vidal, S., Francis, L., Guyot, S., Marnet, N., Kwiatkowski, M., Gawel, R., et al. (2003). The mouth-feel properties of grape and apple proanthocyanidins in a wine-like medium. *Journal of the Science of Food and Agriculture*, *83*(6), 564–573. https://doi.org/https://doi.org/10.1002/jsfa.1394

Vidal, S., Francis, L., Williams, P., Kwiatkowski, M., Gawel, R., Cheynier, V., & Waters, E. (2004). The mouth-feel properties of polysaccharides and anthocyanins in a wine like medium. *Food Chemistry*, *85*(4), 519–525. https://doi.org/10.1016/S0308-8146(03)00084-0

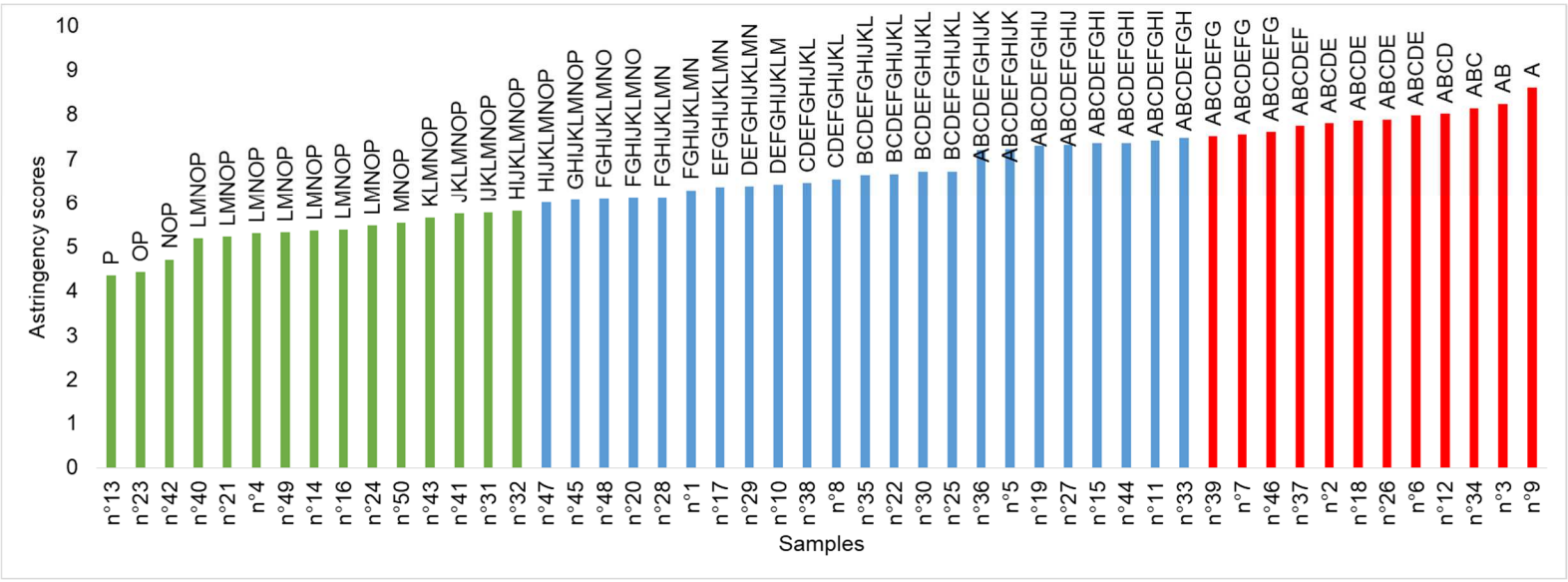
Astringency scores
10
9
8
7
6
5
4
3
2
1
0
P
OP
NOP
LMNOP
LMNOP
LMNOP
LMNOP
LMNOP
LMNOP
LMNOP
MNOP
KLMNOP
JKLMNOP
IJKLMNOP
HIJKLMNOP
HIJKLMNOP
GHIJKLMNOP
FGHIJKLMNO
FGHIJKLMNO
FGHIJKLMN
FGHIJKLMN
EFGHIJKLMN
DEFGHIJKLMN
DEFGHIJKLM
CDEFGHIJKL
CDEFGHIJKL
BCDEFGHIJKL
BCDEFGHIJKL
BCDEFGHIJKL
BCDEFGHIJKL
ABCDEFGHIJK
ABCDEFGHIJK
ABCDEFGHIJ
ABCDEFGHIJ
ABCDEFGHI
ABCDEFGHI
ABCDEFGHI
ABCDEFGH
ABCDEFG
ABCDEFG
ABCDEFG
ABCDEF
ABCDE
ABCDE
ABCDE
ABCDE
ABCD
ABC
AB
A
n°13
n°23
n°42
n°40
n°21
n°4
n°49
n°14
n°16
n°24
n°50
n°43
n°41
n°31
n°32
n°47
n°45
n°48
n°20
n°28
n°1
n°17
n°29
n°10
n°38
n°8
n°35
n°22
n°30
n°25
n°36
n°5
n°19
n°27
n°15
n°44
n°11
n°33
n°39
n°7
n°46
n°37
n°2
n°18
n°26
n°6
n°12
n°34
n°3
n°9
Samples

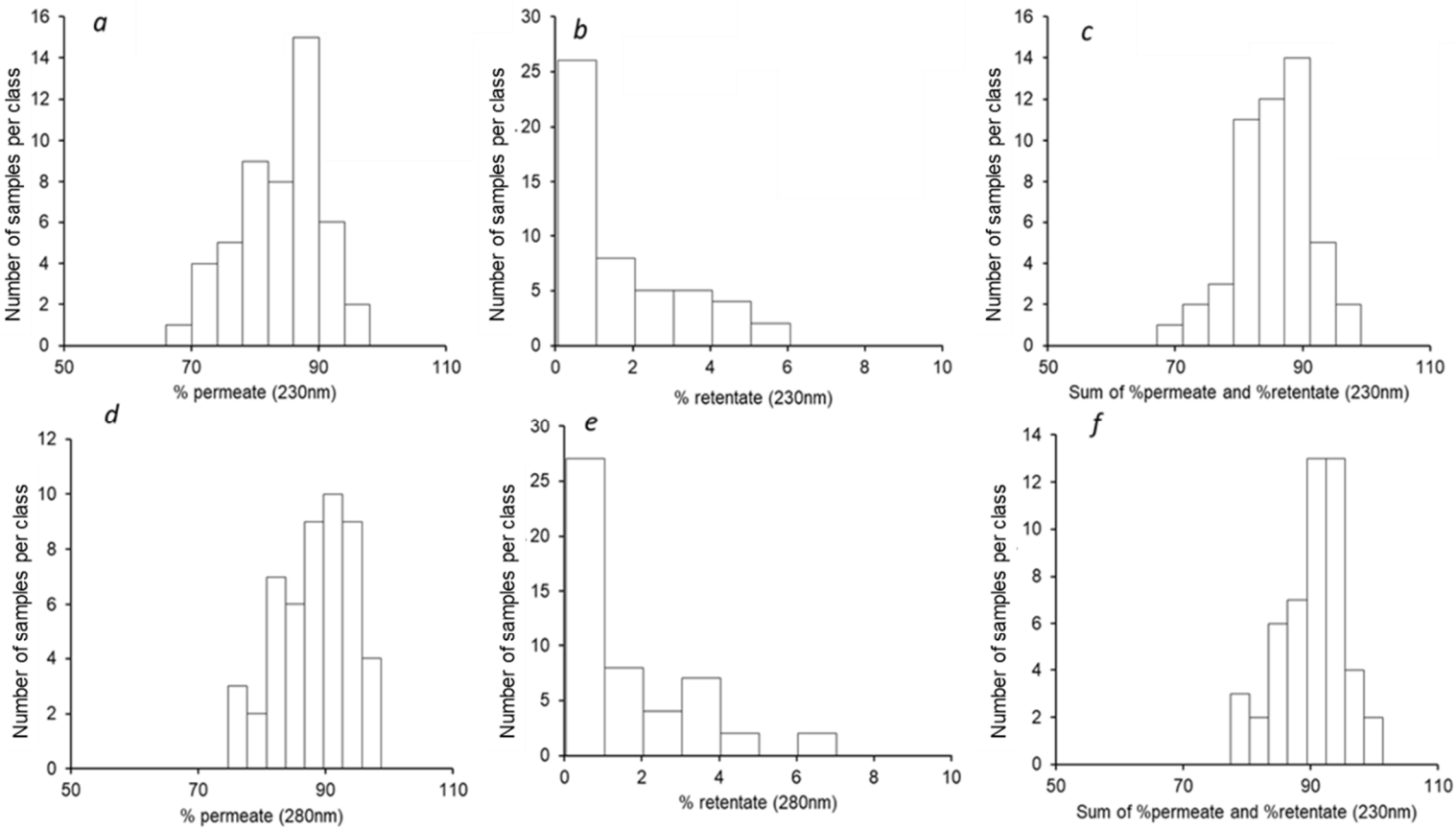
a
Number of samples per class
% permeate (230nm)
b
Number of samples per class
% retentate (230nm)
c
Number of samples per class
Sum of %permeate and %retentate (230nm)
d
Number of samples per class
% permeate (280nm)
e
Number of samples per class
% retentate (280nm)
f
Number of samples per class
Sum of %permeate and %retentate (230nm)

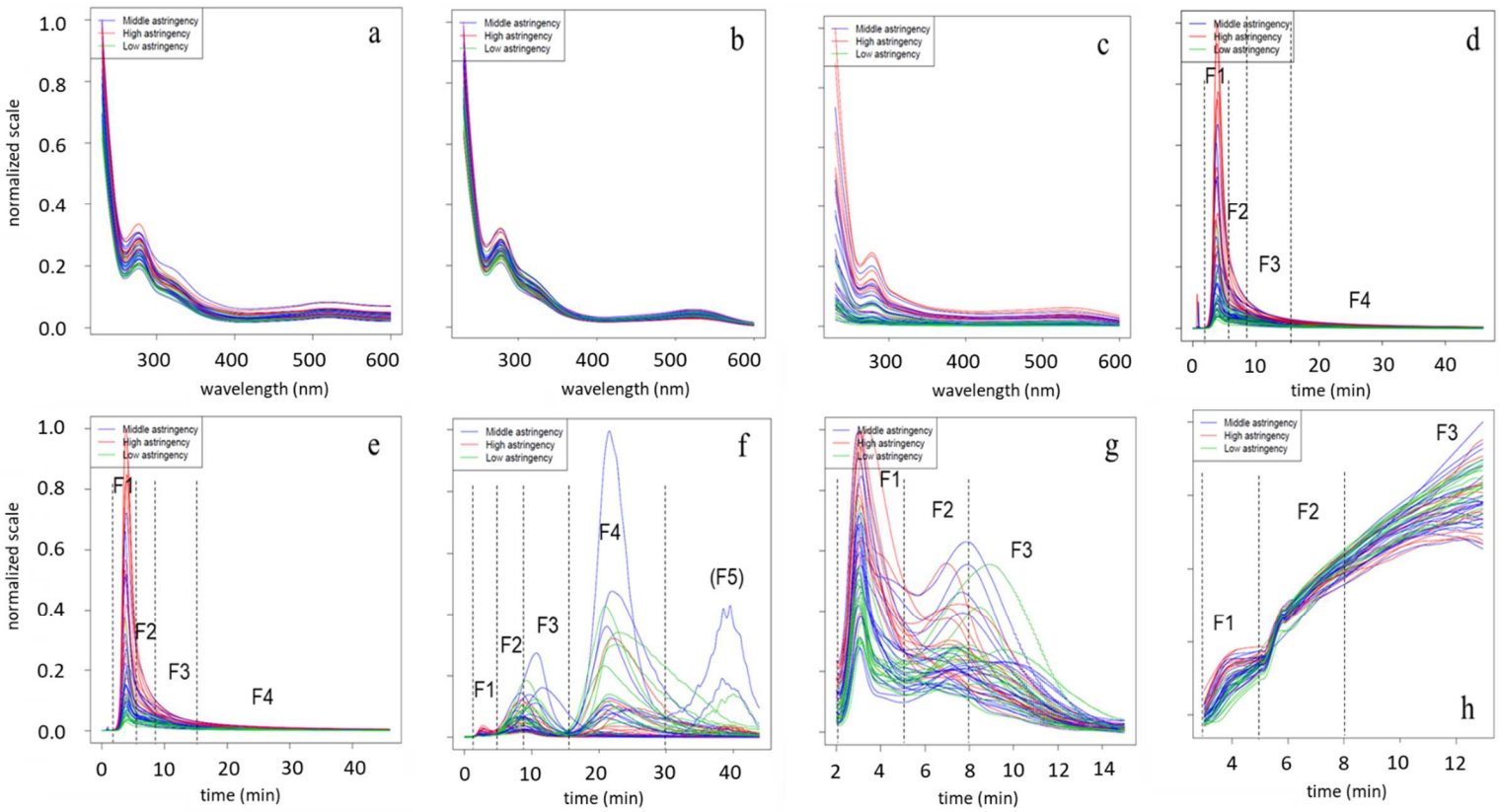
Middle astringency
High astringency
Low astringency
a
b
c
d
e
f
g
h
normalized scale
wavelength (nm)
time (min)
F1
F2
F3
F4
(F5)

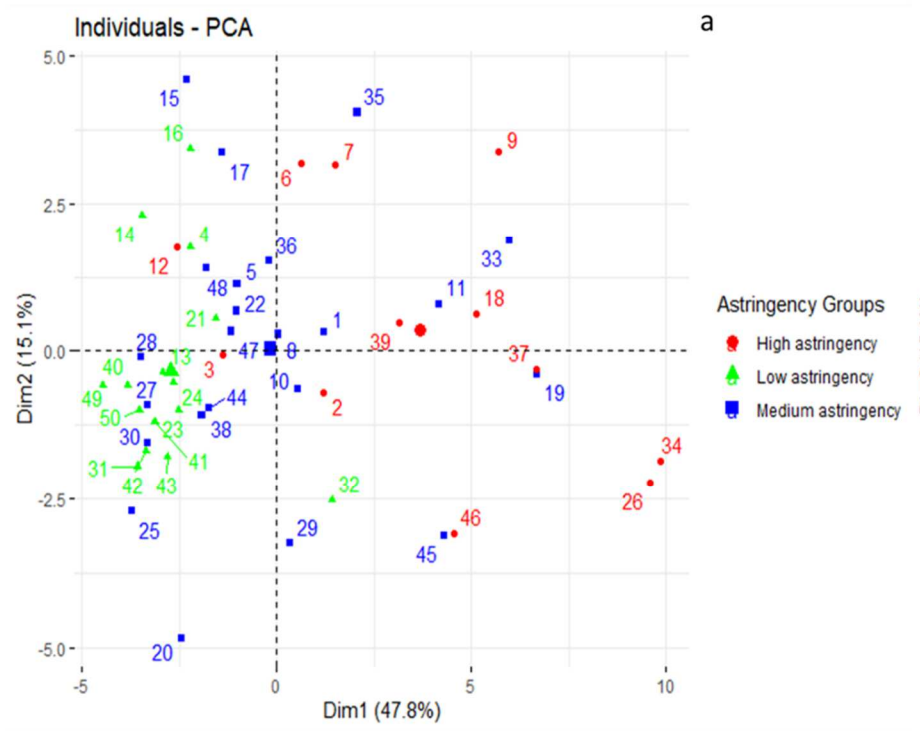
Individuals - PCA
a
Dim2 (15.1%)
Dim1 (47.8%)
Astringency Groups
High astringency
Low astringency
Medium astringency

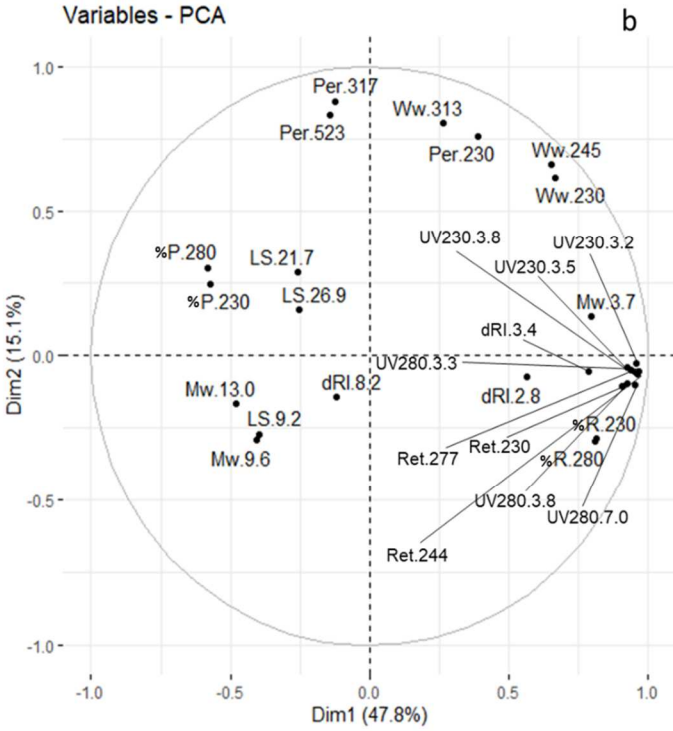
Variables - PCA
b
Dim2 (15.1%)
Dim1 (47.8%)
Per.317
Ww.313
Per.523
Per.230
Ww.245
Ww.230
UV230.3.8
UV230.3.2
UV230.3.5
%P.280
LS.21.7
%P.230
LS.26.9
Mw.3.7
dRI.3.4
UV280.3.3
dRI.8.2
dRI.2.8
Mw.13.0
LS.9.2
Mw.9.6
%R.230
Ret.277
Ret.230
%R.280
UV280.3.8
UV280.7.0
Ret.244

Table 1: Names, contents and dimensions of the ***X*** and ***Y*** tables included in data processing.

	Name	Table	Dimensions (***n*** x ***p***)[a]
X	***X1***	UV fractogram (λ = 280nm)	50 x 5521
	X2	UV fractogram (λ = 230nm)	50 x 5521
	X3	MALS fractogram (angle 90°)	50 x 2551
	X4	dRI fractogram	50 x 821
	X5	Log of weight average molecular weight distribution (Log(M_w))	50 x 592
	X6	UV-vis spectra of retentate fraction	50 x 371
	X7	UV-vis spectra of permeate fraction	50 x 371
	X8	UV-vis spectra of whole wine	50 x 371
Y		astringency score	50 x 1

[a] *n* = number of samples, *p* = number of variables

Table 2: Identification of the three variables selected from each ***X*** table and their corresponding fractions.

Type	***X*** table	Selected variable[a]	Variable name	Corresponding fraction
AF4 fractogram	UV fractogram (λ = 280nm)	3.3	UV280-3.3	F1
		3.8	UV280-3.8	
		7.0	UV280-7.0	F2
	UV fractogram (λ = 230nm)	3.2	UV230-3.2	
		3.5	UV230-3.5	F1
		3.8	UV230-3.8	
	MALS fractogram (angle 90°)	9.2	LS-9.2	F3
		21.7	LS-21.7	F4
		26.9	LS-26.9	
	dRI fractogram	2.8	dRI-2.8	F1
		3.4	dRI-3.4	
		8.2	dRI-8.2	F2
	Log of weight average molecular weight distribution (Log(M_w))	3.7	Mw-3.7	F1
		9.6	Mw-9.6	F3
		13	Mw-13	
UV-vis spectra	UV-vis spectra of retentate fraction	230	Ret-230	-
		244	Ret-244	-
		277	Ret-277	-
	UV-vis spectra of permeate fraction	230	%R 230	-
		280	%R 280	-
		230	Per-230	-
		317	Per-317	-
		523	Per-523	-
		230	%P 230	-
		280	%P 280	-
	UV-vis spectra of whole wine	230	Ww-230	-
		245	Ww-245	-
		313	Ww-313	-

[a]The dimension of variables is the time (min) and wavelength (nm) for the AF4 fractograms and UV-vis spectra, respectively.